

Jets and plumes with negative or reversing buoyancy

By J. S. TURNER

Woods Hole Oceanographic Institution, Woods Hole, Massachusetts†

(Received 15 February 1966)

The motion of turbulent jets of heavy salt solution injected upwards into a tank of fresh water has been compared with that of plumes which are initially buoyant but become heavy as they mix with the environment. The reversal of buoyancy in the latter case is produced by using fluids having a non-linear density change on mixing, a laboratory analogue of the density changes occurring at the top of a cumulus cloud due to evaporation. The behaviour in the two cases is quite different; salt jets reach a steady height about which only small fluctuations occur, while the plumes with reversing buoyancy exhibit violent regular oscillations. This phenomenon, which is clearly a property of the ‘evaporation’ and not just of the geometry, is suggested as a likely explanation of the observed oscillation of the tops of cumulus towers. Dimensional arguments have been used to relate the experimental results to the volume, momentum and buoyancy fluxes at the source. An application of one of the deduced relations to the atmosphere gives realistic periods for the cloud-top oscillations.

1. Introduction

This work has arisen out of an interest in the dynamical behaviour of the tops of cumulus clouds, and in particular the effects that evaporation can have on the mixing and the motion. When a cloud tower is growing upwards into a dry environment, the evaporation of liquid water near the edge causes cooling, and hence a density change. Sometimes a thin layer of dense air produced in this way forms a strong down-draught, which is made visible by the motion of wisps of cloud. The growth of cloud tops is also observed to be unsteady, with the velocity and sometimes the height oscillating in a regular way. It will be found that this phenomenon too can be explained in terms of the density changes due to evaporation.

The essential effect introduced by evaporation is that of the reversal of buoyancy. In the interior of the cloud upward motion is produced because the air there is lighter than the environment, while mixing near the edge can result in the formation of heavier fluid which drives the flow down again. In order to model this process on a laboratory scale, we must use a pair of liquids which exhibit a similar *non-linear* density behaviour when they are mixed. A method of doing this has recently been reviewed elsewhere (Turner 1965), and the technique has previously been used to study the mixing at the top of a stratocumulus

† Present address: Department of Applied Mathematics and Theoretical Physics, University of Cambridge.

cloud (Turner & Yang 1963). This paper is a direct continuation of that earlier work, applied now to a different type of cloud and therefore a different geometry. We shall investigate the properties of a steady plume of buoyant 'non-linear' fluid, initially injected upwards into a large tank of fluid at rest, but free to fall back as its buoyancy is reversed by mixing.

Another question which arose during the course of the experiments is the following: does the behaviour of such a plume really depend on the actual reversal of *buoyancy*, or is it determined entirely by the geometry and the reversal of *velocity* in different parts of the flow? That is, are all the essential properties still the same if we have an upcurrent in the centre, surrounded by an annular downflow, with mixing between these and between the downward flow and the environment? To investigate this point, experiments were also carried out with a jet of salt solution, initially projected upwards against the buoyancy forces by being given excess momentum, and then falling back under gravity.

2. Description of the experiments

The experiments were carried out in a Plexiglas tank 45 cm square in cross-section and 140 cm deep, filled with fresh water. The buoyant fluid was released from a reservoir near the ceiling of the laboratory, connected through a valve and flowmeter to an upward pointing nozzle, which projected from the centre of the bottom of the tank to a height of 50 cm above it. Thus the bottom third of the tank was available to collect the mixture of input and environmental fluid which fell down below the nozzle level, and a given set of experimental conditions could be maintained until this lower part of the tank filled up.

We shall describe first the experiments on the heavy salt jets directed upwards, since their behaviour is perhaps easier to understand. In order to produce enough momentum to force the salt jets upwards, small nozzles (ranging from about $\frac{1}{4}$ in. to $\frac{1}{2}$ in. diameter) were used for all the quantitative experiments. The supply of salt water was suddenly turned on, and then left at a constant setting throughout the run. The first pulse of fluid looked rather like a light starting plume (Turner 1962), with a vortex-like front and nearly steady plume behind. The velocity decreased more rapidly with height, however, and instead of rising indefinitely with a constant shape, the whole plume broadened, came to rest and fell back. Finally it settled down to a nearly steady state, with the top at a lower height than that attained by the first pulse, an upflow in the centre and a downflow surrounding this (see figure 1). Turbulence was then interchanging fluid between the up- and downcurrents, and the mixing of the upflow with heavier descending fluid rather than the stationary environment accounts for the smaller height in the steady state. Fluctuations of this 'steady' height were observed, but these were small and random, comparable with the fluctuations due to large eddies at the side of a plume.

The behaviour of plumes of 'evaporating' fluid was much more dramatic and unexpected. The non-linear density properties of several of the input fluids used, various mixtures of alcohol and ethylene glycol, are shown in figure 2 where they are compared with typical curves for evaporation in the atmosphere; a fuller

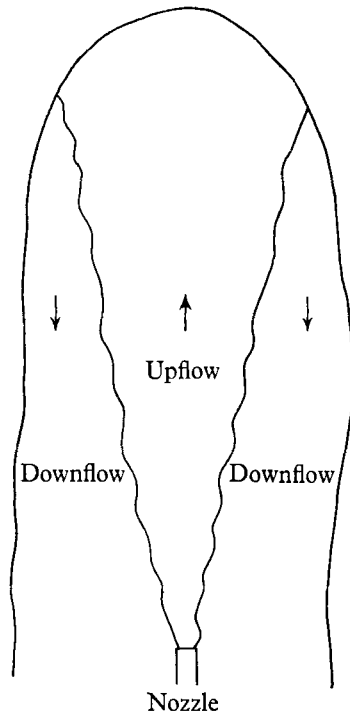


FIGURE 1. Sketch of the up- and downflow regions in a heavy salt jet projected upwards. The outer boundary is approximately to scale, but the inner boundary is schematic only.

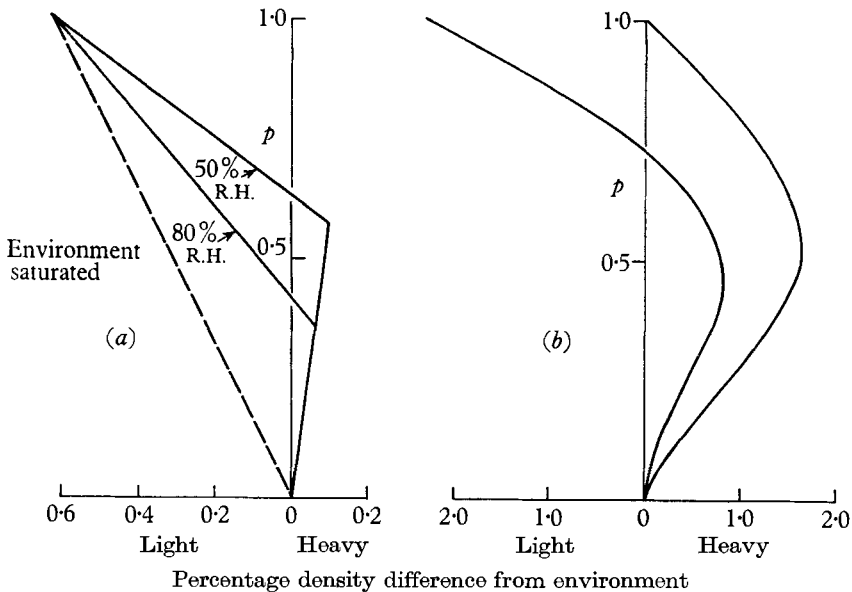


FIGURE 2. The non-linear density behaviour produced when a fraction p of 'cloud' fluid is mixed with its environment. (a) Cloudy air containing 1 g/kg of liquid water mixing with an environment 2 °C cooler having various relative humidities (denoted by R.H. on the figure). Cloud at 2 °C and 700 mb. (b) The experimental plume fluid, consisting of alcohol with ethylene glycol in various proportions, mixing with water.

discussion of this comparison is to be found elsewhere (Turner & Yang 1963) and in § 4 of this paper. Fluid with these properties was released slowly but steadily, usually from a larger nozzle, 4 cm in diameter, to ensure that the upward motion was due to buoyancy and not to injected momentum. The first pulse behaved similarly to the salt jets, rising higher than the mean height at later times, but the subsequent behaviour was completely different. No longer was the height of the top nearly steady with small superimposed fluctuations; instead, it oscillated regularly and with large amplitude. The contrast between two experiments using the same nozzle and in which nearly the same mean height was achieved is shown in figure 3.

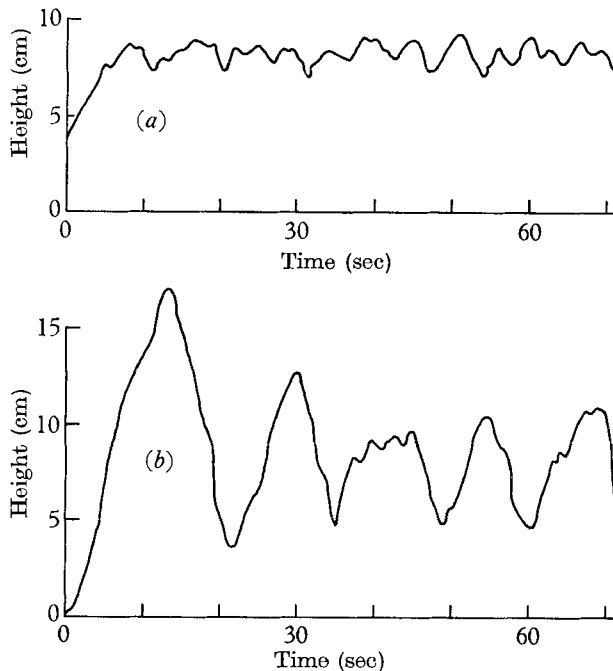


FIGURE 3. The height above a 4 cm diameter nozzle of the top of (a) a salt jet, and (b) a plume of 'evaporating' alcohol-glycol mixture, as functions of time.

A closer examination of these experiments on 'evaporating' plumes suggested that three phases of motion can usefully be distinguished. First, there is the 'starting plume', like those described by Turner (1962) for ordinary buoyant fluids, advancing and growing by mixing over its top and sides. The cap then stops rising while it continues to grow; negative buoyancy is being accumulated at this stage, but downward motion is small. Finally, the cap as a whole collapses, sometimes even developing a reversed circulation like that in a downward moving thermal. This temporarily cuts off the supply of buoyant fluid from below, but a new cap breaks through and the cycle begins again. Some of these features are shown in the photographs of figure 4 (plate 1) and this general picture will be used in developing the theoretical model of § 4.

The marked differences between the salt jets and 'evaporating' plumes can be understood qualitatively if we think of the distributions of vertical velocity

which must be produced in the two cases. The momentum driven salt jets will always have their maximum upward velocities concentrated over a small cross-section near the nozzle. The velocity will fall gradually to zero, reverse at the maximum height, and then after a short period of acceleration the velocities in the downward-moving annular region will again be decreasing with distance. These downward velocities can therefore never become large enough to cut off completely the upward flow from the source. The ‘evaporating’ plumes, on the other hand, start with *low* upward velocities; they are accelerated upwards by buoyancy, and then undergo a rapid reversal of buoyancy as they mix. The accumulation of downward buoyancy at this stage allows quite large velocities to be developed in the thermal-like element which results; these can evidently become greater than the upward velocity near the source, and so the supply of buoyant fluid can be cut off.

There can of course be a continuous transition between the two types of behaviour. If a fixed flux of ‘evaporating’ fluid is ejected with higher and higher velocities so that the externally imposed momentum becomes more important than that produced by the upward buoyancy force, then the height attained increases, and the amplitude of the oscillations decreases until they are lost in the random fluctuations characteristic of the jets. In general, momentum-driven salt jets can extend to many nozzle diameters above the source, whereas turbulent ‘evaporating’ plumes will not. Motion driven entirely by buoyancy can only reach greater heights if it is laminar near the exit nozzle, as was the case in the previously published photographs of Turner (1965). In the more detailed experiments and theory presented here we will consider only fully turbulent jets and plumes.

3. Heavy jets injected upwards

With the behaviour described in the previous section as our guide, we can now explore some of the properties of the steady turbulent salt jets using dimensional arguments. We would expect, first, that the patterns of up- and downflow produced by a small source should remain geometrically similar for all conditions of the outflow. The shape of the flow is sketched in figure 1. The outer boundary of the downflow in this figure is to scale, and represents the mean position of the edge as recorded on many photographs. It is nearly cylindrical, with a rounded cap, and the mean height above the source is just twice the diameter. The inner boundary is schematic only, since detailed interior measurements have not been made, but it is unlikely to differ much from a cone, except perhaps near the cap. This line of zero mean motion could be traced more precisely if required, using the method described by Rouse (1956) for the similar case of a jet in a counterflow.

Just two parameters define the flow from a small (effectively point) source: the momentum flux M and the (negative) buoyancy flux F_2 (both divided by ρ to remove the dependence on mass). All the properties of the flow can be scaled in terms of combinations of these two. In particular the height of the top should be of the form

$$z_m = CM^{\frac{3}{2}}F_2^{-\frac{1}{2}}, \quad (1)$$

where C is a constant. We suppose that the momentum and buoyancy fluxes are

produced by ejecting fluid with density ρ into a fluid at rest (density ρ_1), with the volume flux V and velocity u from a small nozzle, radius r . As is usual in such problems, density differences will be neglected except in the buoyancy terms. If the turbulent velocity profile across the cylindrical outlet is approximated by a uniform velocity, then

$$\begin{aligned} V &= \pi r^2 u, & M &= \pi r^2 u^2 & F_2 &= \pi g \frac{(\rho - \rho_1)}{\rho_1} r^2 u \\ & & & & &= \pi^{-1} r^{-2} V^2, & &= \Delta V \quad \text{say.} \end{aligned} \quad (2)$$

Inserting (2) in (1) gives

$$z_m = C \pi^{-\frac{3}{2}} V \Delta^{-\frac{1}{2}} r^{-\frac{3}{2}}. \quad (3)$$

It is in this form that the result (1) will be tested experimentally.

One could in the same way evaluate the velocity or time scales for this flow, but since the final state is observed to be steady, these will have no particular significance here.

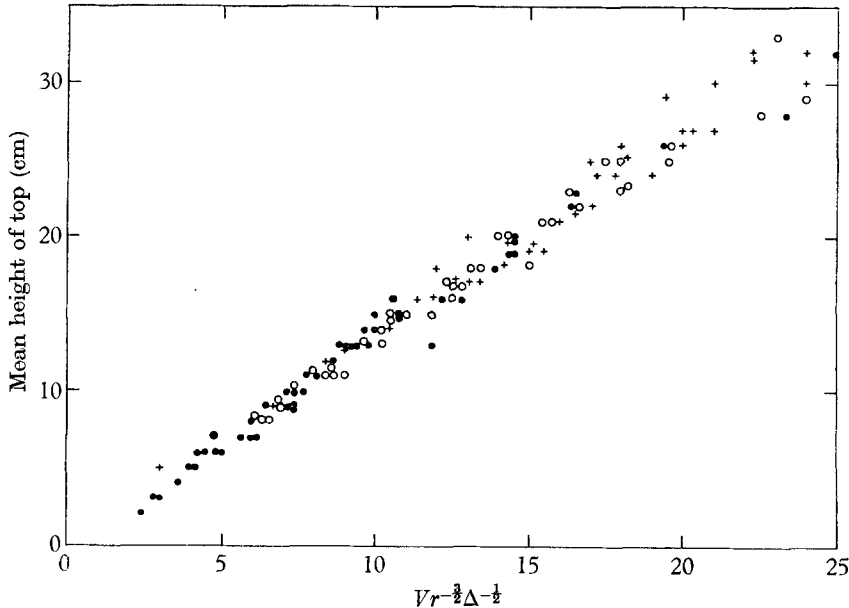


FIGURE 5. Measured mean heights of the tops of salt jets projected upwards compared with the form suggested by the dimensional arguments. The symbols refer to different nozzle diameters: ●, 1.40 cm; ○, 0.96 cm; +, 0.65 cm.

A large number of individual experiments on heavy salt jets in water was performed, using three nozzle sizes and a wide range of volume fluxes and initial density differences. Both the initial height of rise and the steady mean height were estimated to the nearest centimetre against a marker wire next to the jet. The mean height is plotted in figure 5 against the form suggested by (3), and it is seen that there is good support for the dimensional result. There seems to be no systematic 'virtual source' effect for different nozzle sizes, and actual heights above the outlet have been plotted in figure 5. The constant C evaluated from

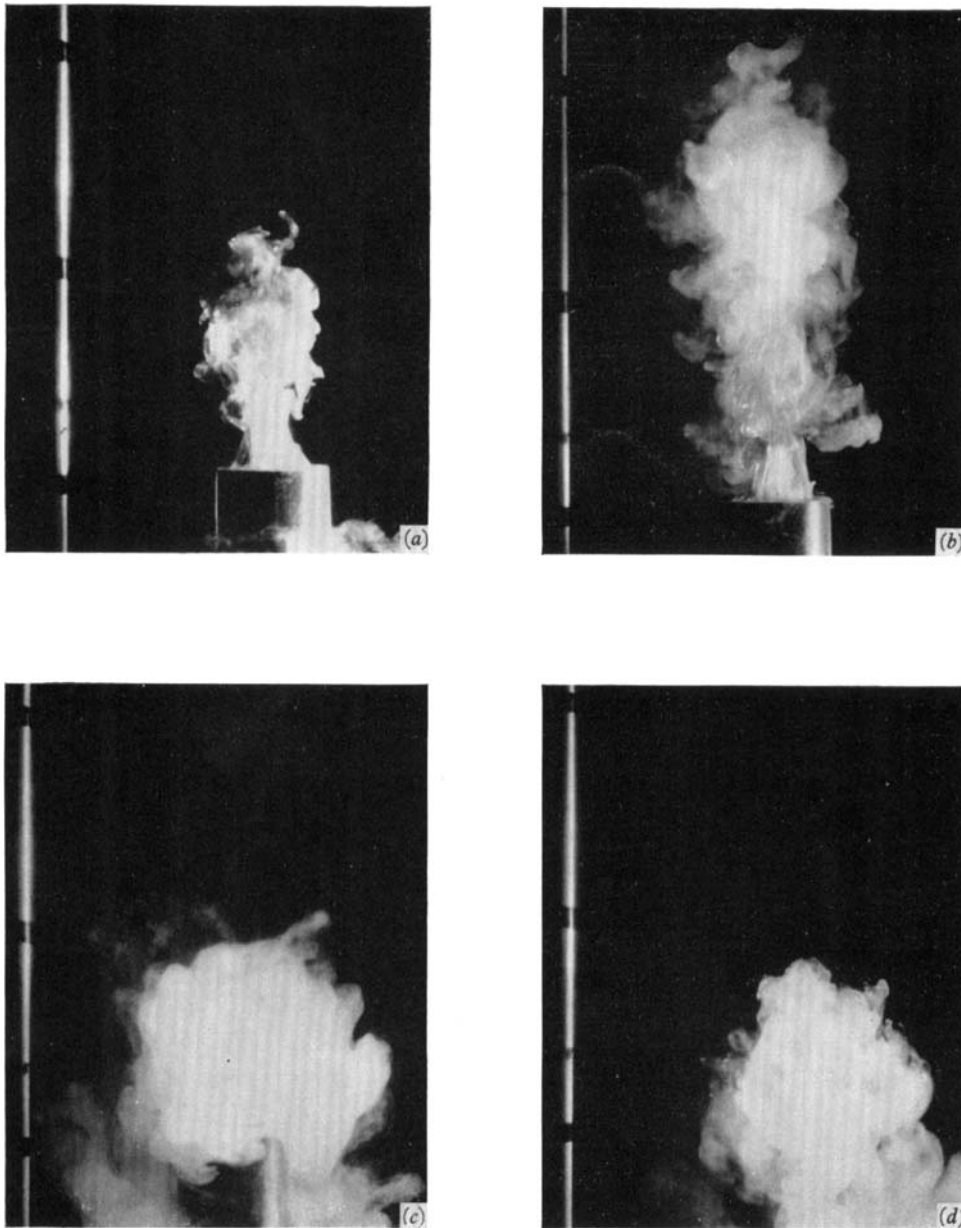


FIGURE 4. Photographs showing the various stages of growth and decay of an 'evaporating' plume described in the text: (a) the motion begins like a 'starting plume'; (b) negative buoyancy accumulates in the cap; (c) the plume collapses; (d) a new 'tower' begins to break through. Throughout the experiment the output of light fluid is of course continued at a constant rate. The successive pictures are separated by about 5 sec; the height markers on the left are 10 cm apart.

the line drawn to fit these experiments is 1.85. The ratio of initial height to steady height varied only within a narrow range, with a mean value over all experiments of 1.43.

It should be possible to set up a detailed theory of this motion, in the manner suggested by Morton (1962) for coaxial turbulent jets with no density differences. Such a theory, combined with the present experimental results, could shed light on the nature and magnitude of the interchange between the turbulent up- and downflows, about which little is known at present.

4. Plumes with reversing buoyancy

(a) *Theoretical arguments*

The parameters governing the behaviour of plumes with a non-linear density behaviour are not so obvious, and will require more discussion. We have chosen to express the results in terms of the initial *volume* flux V_1 of fluid from the source, and two *buoyancy* fluxes, the initial flux F_1 upwards and the ‘asymptotic’ flux F_2 downwards, where F_2 is strictly the flux which would be achieved on infinite dilution. The motion could in principle depend also on the details of the intervening non-linear density behaviour, but in all the experiments reported here the dilutions achieved in the plume before it started to descend were so large that the buoyancy flux during the whole of the downward motion was effectively F_2 . The volume flux at first sight appears to be a redundant parameter, since ordinary plumes can be defined by virtual sources of buoyancy alone, but it is essential here because the density at any time depends on the ratio of ejected volume to that of the total mixture: a zero volume flux initially would imply a constant negative buoyancy flux. This too is the underlying reason for using larger nozzle sizes, and it will be assumed (initially at any rate) that the radius of the source as such is not an important parameter for the system.

The characteristic height z , radius b and time scale t associated with the reversing plumes can be written in terms of these three parameters in the form

$$\left. \begin{aligned} b, z &= V_1^{\frac{2}{3}} F_2^{-\frac{1}{3}} f_{1,2}(R), \\ t &= V_1^{\frac{2}{3}} F_2^{-\frac{2}{3}} f_3(R). \end{aligned} \right\} \tag{4}$$

Here f_1 , f_2 and f_3 are functions of the (non-dimensional) ratio of the final to the initial buoyancy fluxes $R = F_2/F_1$. As in (2) of the previous section, we can relate the buoyancy and volume fluxes through a density difference, or Δ_2 say, defined by

$$F_2 = \Delta_2 V_1. \tag{5}$$

Δ_2 is thus the (fictitious) buoyancy force which would be associated with the asymptotic buoyancy flux if the volume flux remained constant at V_1 . It is shown in figure 6, which is discussed further in the following section. Hence (4) can be written

$$\left. \begin{aligned} b, z &= V_1^{\frac{2}{3}} \Delta_2^{-\frac{1}{3}} f_{1,2}(R), \\ t &= V_1^{\frac{2}{3}} \Delta_2^{-\frac{2}{3}} f_3(R), \end{aligned} \right\} \tag{6}$$

and for an input fluid of fixed properties we could examine the dependence on V_1 alone.

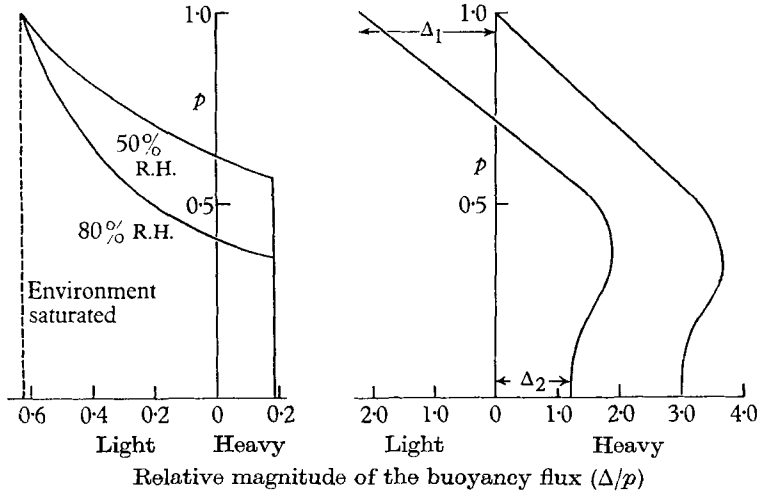


FIGURE 6. The change in buoyancy flux associated with mixing between atmospheric and model clouds and their environments. This figure replots the data of figure 2 in a different form.

A detailed solution of the problem (which is not attempted here) is of course required to find the dependence of b and z on time, but guided by the observations, we can now identify the forms (4) or (6) with the mean height, size and period τ of oscillation. It is convenient for some purposes to eliminate V_1 between (4) or (6) and to express the period in terms of an observed mean height or diameter; for example

$$\left. \begin{aligned} \tau &= z^{\frac{1}{2}} F_2^{-\frac{1}{2}} f_4(R), \\ \text{or} \quad \tau &= z^{\frac{1}{2}} \Delta_2^{-\frac{1}{2}} f_5(R). \end{aligned} \right\} \quad (7)$$

The results of the laboratory experiments will show, in fact, that the major effects are explained by variations of V_1 and F_2 (or z and Δ_2) alone, and that R is of secondary importance over the range of this parameter we are able to cover.

The arguments up to this point have been developed in such a way as to show how z and τ separately depend on the properties of the plume which can be controlled at the source. The relations (7) between the two experimentally derived quantities z and τ can however be obtained more directly and perhaps made more plausible by using a simple mechanistic argument based on the observed behaviour discussed in § 2. Suppose that the steady negative buoyancy flux F_2 feeds into the thermal-like cap for a time $\frac{1}{2}\tau$, so that the total buoyancy accumulated in this time is $B = \frac{1}{2}F_2\tau$. When this region of negatively-buoyant fluid descends, its velocity will be of order $B^{\frac{1}{2}}d^{-1}$, where d is its mean diameter (see, for example, Scorer 1957). It will travel a distance z comparable with its diameter d in a time $d^2B^{-\frac{1}{2}}$. If this time of descent is approximately equal to the accumulation time (as it is observed to be in practice) then

$$\frac{1}{2}\tau = B/F_2 \approx z^2B^{-\frac{1}{2}}. \quad (8)$$

Eliminating B and substituting back in (8) gives an estimate for the period

$$\tau \approx z^{\frac{1}{2}} F_2^{-\frac{1}{2}}. \quad (9)$$

This is of the form (7); the constant of proportionality can of course in principle depend on the parameter R which was neglected in the above argument, through its effect on the geometry of the oscillating plume, i.e. the relation between the height achieved and the maximum radius.

(b) *Properties of the non-linear fluids*

Before the detailed experimental results are presented, something more should be said about the character of the density non-linearity of the fluids used, and the method employed to evaluate Δ_2 , or the equivalent asymptotic downward buoyancy flux. In figure 6 the data shown in figure 2 have been replotted, but now with Δ/p , which is proportional to the buoyancy flux, along the abscissa instead of Δ . The interpretation of 6(a), for the case of the cloud, is straightforward. As mixing proceeds, the upward buoyancy flux is reduced, falls to zero and then reverses. When all the liquid water has evaporated the downward flux becomes a maximum, and it maintains this value whatever the further dilution with environmental air. For the mixtures of alcohol and ethylene glycol shown in 6(b), the density behaviour on dilution with water is more complicated: the downward buoyancy flux reaches a maximum at an intermediate value of p , and then decreases again towards its asymptotic value. This effect is of course associated with the reversal of curvature in the density curves of figure 2; it was not found in the previous experiments (Turner & Yang 1963), probably because there two different mixtures of alcohol and water with potassium iodide dissolved in one of them were used as the initial fluids, rather than the alcohol-glycol and pure water used here.

Curves such as those shown for illustration in figure 6(b) were prepared covering the whole range of alcohol-glycol mixtures for which buoyancy reversal is possible. These were used to relate the density of the input fluid to the asymptotic buoyancy flux, so that during the actual experiments a single weighing of a relative density bottle was sufficient to define Δ_2 using this calibration. The form of the non-linearity obtainable in this way was very limited, since the variations which can be obtained with various alcohol-glycol mixtures amount to a shifting of the curves of figure 6(b) sideways, with a systematic change in horizontal scale. However, a large range of values of R , or ratio of final to initial buoyancy fluxes, can be achieved by this means, with density differences and non-linear effects somewhat larger than typical for the atmosphere. One could perhaps also explore the properties of various three-component systems, but it was found that the odd behaviour of the downward buoyancy flux did not present any special problems of interpretation. The experimental data were tentatively plotted using the maximum downward flux as an alternative parameter to the asymptotic value: the latter was clearly the more effective in ordering the data, and has been used in all the figures presented here. That this should be so is also obvious when the experiments are examined in more detail, since downward motion usually begins only when the total volume of input fluid has been increased at least ten times by mixing, thus bringing the buoyancy flux well below the maximum and towards the asymptotic value. The strong dependence on Δ_2 , rather than on the details of the non-linear behaviour at intermediate dilutions, also makes it more

likely that the laboratory results can give useful predictions for the atmospheric clouds, in spite of the differences in the detailed non-linear behaviour shown in figure 6.

(c) *Experimental results*

Experiments were carried out over as wide a range of parameters as possible, using a 4 cm diameter nozzle (unless otherwise mentioned) to ensure that the upward motion was driven by buoyancy. The volume flow rate V_1 was varied by a factor of 30, from about 1.2 to 35 cc/sec, and Δ_2 ranged between 5 and 25 cm sec⁻². Experiments with lower values of Δ_2 were not very repeatable, possibly because of the large difference between the maximum and asymptotic fluxes. When the input fluid becomes so light that Δ_2 just changes sign, a curious double buoyancy reversal is possible (see figure 6), and was observed: as dilution continues the plume fluid goes up, down, and then up again. Experiments in which this behaviour was observed are not included in the following figures. At the larger values of Δ_2 and small V_1 , the plumes tended to be laminar; and in order to avoid this and extend the range of experimental conditions, a nozzle 1.4 cm in diameter was used where indicated in figure 8.

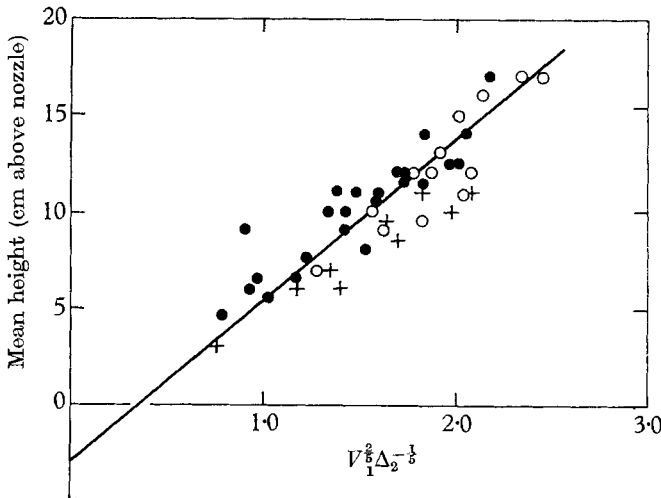


FIGURE 7. The measured mean heights of the tops of plumes of alcohol-glycol mixtures released from a 4 cm diameter nozzle, compared with the form suggested by dimensional arguments. The symbols refer to different ranges of the buoyancy ratio, R , or different Δ_2 . ●, $R < 0.5$, $\Delta_2 \leq 10$; ○, $0.5 \leq R \leq 1.5$, $10 < \Delta_2 < 20$; +, $R > 1.5$, $\Delta_2 \geq 20$.

The first third of the runs were recorded photographically, covering at least four periods of the oscillatory motion, and the mean period τ , mean height z_m of the top above the nozzle and the diameter d at the mean height measured off the film. Later experiments were made visually, timing the oscillations over about ten periods with a stopwatch, and recording at the same time the maximum and minimum heights. Both time and height measurements were not always obtained in the same runs. In figure 7 are shown the mean heights plotted against the parameter $V_1^2 \Delta_2^{-1/2}$ suggested by the relation (6). The different symbols refer to

different ranges of Δ_2 (or R) as described in the caption, and it can be seen that there is some indication of a small systematic dependence on R , the ratio of the final to the initial flux. The differences are barely outside the experimental scatter, and a single line has been fitted by eye to all the points, which has a slope of 8.4 and a negative intercept on the height axis of 3 cm. This 'virtual source' effect is small, and the experimental results do not rule out a line through the origin with a slightly lower slope. The results are accurate enough, however, to confirm that the height attained depends much less strongly on V_1 than it does for the heavy salt jets shown in figure 5.

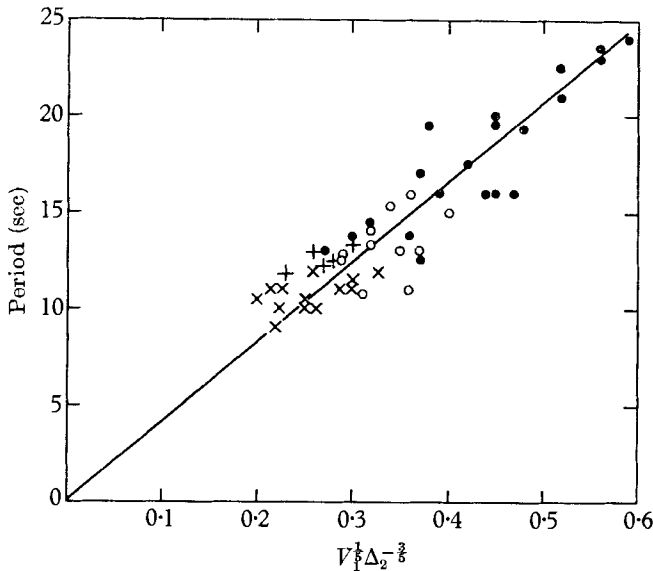


FIGURE 8. The measured periods of the oscillating tops of alcohol-glycol plumes compared with the form suggested by the dimensional theory. Three of the symbols refer to the same conditions as in figure 7. The extra symbol \times is used for experiments with a nozzle 1.4 cm diameter.

The experimentally determined periods are shown in figures 8 and 9. In figure 8 they have been plotted against $V_1^{1/2} \Delta_2^{-3/2}$ as suggested by (6). Some results with a smaller nozzle are also plotted here, and these too seem to be well represented by the dimensionally chosen form. Figure 9 shows the period as a function of $z^{1/2} \Delta_2^{-1/2}$, suggested by (7), where $z = z_m + 3$ is the distance above the virtual origin. All the runs in which both the periods and heights were measured have been used for this purpose. Again the representation of the experiments by this function is fairly good, and if we neglect a possible systematic dependence on R , the constants of proportionality can be estimated to give

$$\begin{aligned} \tau &= 41 V_1^{1/2} \Delta_2^{-3/2} \\ &= 14 z^{1/2} \Delta_2^{-1/2}. \end{aligned} \tag{10}$$

The slope of the line drawn through the points in figure 9 is consistent with the appropriate combination of those in figures 7 and 8. The numerical values are

little changed by any reasonable choice of lines to fit the experimental points, for instance a line through the origin in figure 7.

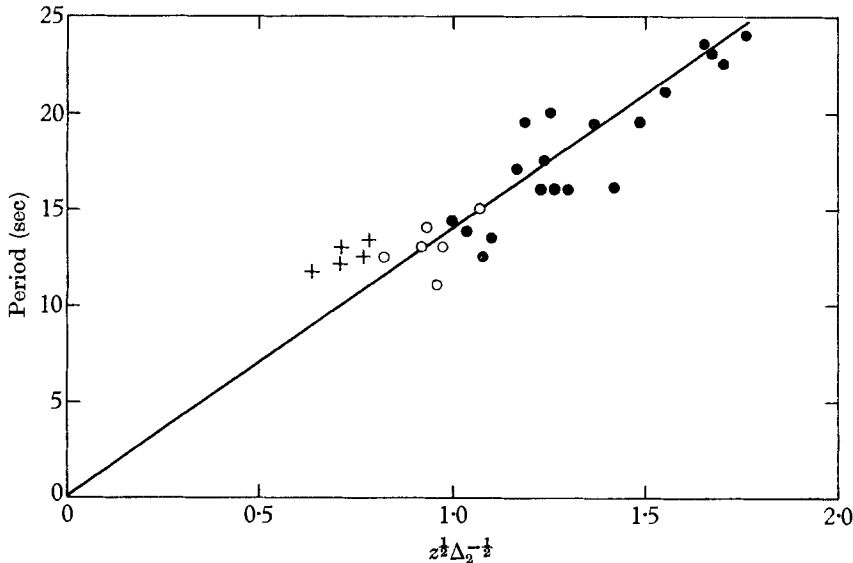


FIGURE 9. The measured periods of model cloud-top motions, plotted against a function of the measured height z above a virtual source and the properties of the plume fluid. The symbols refer to the same ranges of R or Δ_2 as in figure 7.

5. Discussion

The main result of these experiments is a qualitative one: it has been demonstrated that there is an essential difference between the behaviour of jets and plumes in which the motion is first up and then down, depending on the mechanism by which the upward motion is generated. Jets in which the buoyancy forces always act downwards, and which must therefore be driven upwards by momentum at the source, reach a steady height and fluctuate randomly and with small amplitude about this. Plumes accelerated upwards by buoyancy which then reverses on mixing are found to have a regular oscillatory behaviour, with large-amplitude fluctuations of the height of the top. Through dimensional arguments some further understanding of the phenomena has been obtained, and the relations suggested theoretically have received good support from the laboratory experiments.

Even the qualitative result, however, sheds light on the atmospheric phenomenon we set out to study, the oscillation of the tops of cumulus clouds. Previous explanations of such observations have been of two kinds. It was supposed by Scorer & Ludlam (1953) (and others) that the rise and fall of cloud towers is evidence of an intermittent release of buoyant 'bubbles' or thermals from cloud base, and that each pulse is associated with the arrival of a new thermal at the top of the cloud. Workman & Reynolds (1949), on the other hand, pointed to the regularity of some cloud top motions, with nearly equal times of rise and fall over many cycles, and it seemed unlikely that this could be explained by an unsteady

process. Priestley (1953) showed that the observed periods are roughly consistent with an oscillation of a buoyant element in the stably-stratified environment of a cloud. The experiments described here reveal another possibility, however, since regular oscillations are obtained in our model with a *steady* source and *neutral* stratification of the surroundings. Oscillations of cloud tops could arise purely as a consequence of the gradual build up and collapse of regions of cold, negatively buoyant air which are formed by evaporation as dry air is mixed into the cloud.

The model experiments also allow us to make quantitative predictions for the atmosphere, and to compare these predictions with those of Priestley. It is convenient first to convert (10) into an expression involving the cloud diameter, rather than the height. To do this we have used the smaller number of photographed runs, for which values of the diameter at the mean height can be measured, and find that $d = 0.6z$ approximately; so (10) becomes

$$\tau = 18d^{\frac{1}{2}}\Delta_2^{-\frac{1}{2}}. \quad (11)$$

Plausible values for the diameter and temperature difference do indeed lead to realistic periods using (11): if one takes a temperature difference of about 2°C or $\Delta_2 = 8$, say, and a tower diameter $d = 300m = 3 \times 10^4 \text{ cm}$, then

$$\tau \approx 10^3 \text{ sec} \approx 15 \text{ min},$$

which is characteristic of the periods observed. Priestley, on the other hand, used the Brunt-Väisälä period

$$\tau = 2\pi \left(\frac{g}{T_p} \frac{\partial T_p}{\partial z} \right)^{-\frac{1}{2}} = 2\pi \left(\frac{\partial \Delta_e}{\partial z} \right)^{-\frac{1}{2}}, \quad (12)$$

where T_p and Δ_e are the potential temperature and the buoyancy parameter associated with the environment. Equations (11) and (12) are, of course, of the same form dimensionally, but the length and density differences entering are quite different. Since in typical conditions they both seem to give reasonable values for the period, the question of mechanism can only be resolved by a more careful measurement of all the parameters in circumstances when oscillations are observed. To test the suggestion made in this paper, we should look for an oscillatory behaviour under conditions when the atmosphere is nearly neutrally stable, but there is dry air aloft. Dr Claës Rooth has suggested in private discussion that perhaps the largest, most regular oscillations occur when (11) and (12) imply the *same* period, so that a resonant interaction between the two mechanisms becomes possible.

A question which has not been treated here is the oscillation of the upward velocity of a cloud top while it continues to grow upwards, which is more frequently observed than an oscillation about a steady height (for example, see Anderson 1960). It seems likely that this behaviour too could be explained in terms of the effect of evaporative cooling acting on an updraught of gradually increasing intensity. Experimentally one should seek to produce a model in which analogues of both condensation and evaporation are present simultaneously, but a satisfactory method of doing this has not so far been found.

This is Contribution No. 1771 from the Woods Hole Oceanographic Institution, and has been supported under Contract no. 2196 from the Office of Naval Research. Part of the work described here was presented at the International Conference on Cloud Physics, held in Tokyo in May 1965.

REFERENCES

- ANDERSON, C. E. 1960 *AFCRL Geophysical Research Paper*, no. 72.
MORTON, B. R. 1962 *Int. J. Heat Mass Trans.* **5**, 955.
PRIESTLEY, C. H. B. 1953 *Aust. J. Phys.* **6**, 279.
ROUSE, H. 1956 *Proc. Amer. Soc. Civil Eng., Hyd. Div.* **82**, 1038-8.
SCORER, R. S. 1957 *J. Fluid Mech.* **2**, 583.
SCORER, R. S. & LUDLAM, F. H. 1953 *Quart. J. Roy. Met. Soc.* **79**, 94.
TURNER, J. S. 1962 *J. Fluid Mech.* **13**, 356.
TURNER, J. S. 1965 *Weather* **20**, 124.
TURNER, J. S. & YANG, I. K. 1963 *J. Fluid Mech.* **17**, 212.
WORKMAN, E. J. & REYNOLDS, S. E. 1949 *Bull. Amer. Met. Soc.* **30**, 359.